High-resolution low-energy electron reflection from W(100) using the electron energy-loss spectrometer: A step towards quantitative analysis of surface vibrational spectra

J. P. Woods and J. L. Erskine
Department of Physics, University of Texas, Austin, Texas 78712

(Received 31 October 1986; accepted 8 Decmeber 1986)

High-resolution low-energy electron reflection measurements and electron energy-loss measurements for clean W(100) and for the hydrogen saturated phase (β_1) on W(100) are reported. The ability to perform both low-energy reflectance, low-energy electron diffraction, and high-resolution electron energy-loss experiments on the same crystal using the same electron optics permits several novel experiments. For example, it is possible to quantitatively test the dipole scattering mechanism and examine dipole and impact loss cross sections under precisely defined scattering conditions (i.e., under diffracted beam emergence conditions or at energies corresponding to reflectance resonance conditions). Under certain scattering conditions, the "dipole" scattering selection rule is shown to break down. Suitable modifications of the electron optics control electronics also permit direct measurements of the cross-section energy dependence of vibrational losses. These new features represent an important step towards quantitative applications of vibrational spectroscopy based on comparing electron energy-loss spectroscopy signals from chemisorbed species on different crystal surfaces.

I. INTRODUCTION

Elastic and inelastic scattering of electrons from crystals provides an extremely important probe of their surface properties. Low-energy electron diffraction (LEED) is a well known and widely used structural probe, and high-resolution electron energy-loss spectroscopy (EELS) is now well established as one of the most useful probes of surfaces. Low-energy electron reflectance from crystal surfaces is a third electron based probe capable of yielding important information about surfaces; however, application of this technique is not as widespread as LEED or EELS. One common feature of all three of these techniques is that they all require similar capabilities in the electron beam source and the detection. Therefore, in principle, all three spectroscopic techniques can be carried out using the same instrument, in particular, a suitably modified EELS spectrometer. Used together, the three techniques constitute a useful and complementary group of surface probes.

Interest in the low-energy reflectance of electrons from crystal surfaces stems from the sharp intensity fluctuations as a function of electron energy which are observed. Reflection fine structure is observed below the energy thresholds at which diffracted beams emerge from the surface. The fine structure is attributed to interference between the preemergent beam, which suffers a backreflection from the surface barrier, and the wave directly reflected by the atomic planes. The approximate d^{-1} dependence of the surface potential yields fine-structure fringes in the reflectance which exhibit characteristics of a Rydberg-like dispersion law and which converge at the emergent beam thresholds.

McRae[1] and others[2–4] have carried out extensive studies of low-energy electron reflectance fine structure, and various theoretical descriptions have evolved which account fairly well for the experimental observations. The low-energy reflectance data alone serve as useful probes of the surface potential, and also as tests of LEED calculation procedures at very low energies. The surface potential also plays a key role in proper descriptions of work functions, surface vibrations, and phenomena involving electron emission. However, our primary interest in the present discussion is focused on the relationship between reflectance data and EELS experiments and possible uses of the combined techniques.

Electron reflectance properties of crystals are important in relation to the underlying mechanisms of high-resolution electron loss spectroscopy. One example of this property is illustrated by considering the dipole scattering mechanism,[5–10] which forms the basis for observing surface vibrational losses in specular scattering geometry. Dipole scattering can be viewed as a combination of elastic reflection from the surface followed or preceded by an inelastic loss. Because of this factorization of the scattering cross section, surface electron reflectance behavior is expected to play an important role in determining vibrational loss cross sections produced by the dipole scattering mechanism. Under certain scattering conditions, a null in the electron reflectance can lead to a breakdown in the "dipole" scattering selection rule which is commonly used to identify vibrational modes normal to the surface. A second example, which serves to illustrate the potential importance of electron reflectance behavior in relation to applications of EELS as a structure-sensitive probe, involves the potential breakdown of impact scattering pseudoselection rules.[11] In this case, rapid variation of the electron reflectance, which accompanies surface scattering resonances or LEED beam emergence, can invalidate assumptions required to derive certain scattering cross-section selection rules in the large momentum transfer regime. A third situation in which accurate information about the reflectance behavior of surfaces is important in relation to EELS experiments arises when one wishes to compare the

 0734-2101/87/040435-05$01.00

vibrational cross sections of a particular adsorbed atom or molecule on two different surfaces [(100) and (110), for example] of the same crystal. These are issues which we wish to address in our present discussion.

II. EXPERIMENT

The experiments described in this paper were performed on clean and hydrogen saturated W(100) surfaces. This particular surface and its interaction with hydrogen exhibits a rich variety of phenomena which are described in detail elsewhere.[12–16] For the purpose of the present discussion, it is sufficient to note that the properties of β_1H on W(100) are well established. The β_1H phase consists of two bridge bonded hydrogen atoms per tungsten surface unit cell.[17] LEED,[18] first-principles calculations, and analysis of vibrational energies[19] have established that the height of β_1 hydrogen atoms on W(100) is approximately 1.17 Å above the surface plane. The tungsten surface crystal structure is stabilized to a (1×1) structure by the saturated hydrogen overlayer. Ion channeling[20] has established that there is no measurable lateral displacement of W surface atoms for the β_1H stabilized (1×1) structure. The clean room-temperature W(100) surface is unstable and is believed to be disordered, and upon cooling reconstructs by the condensation of an M_5 phonon displacement yielding a $c(2\times2)$ structure.[14] Vibrational properties of β_1H on W(100) have been extensively studied.[17,21,22] Vibrational energies of the three fundamental modes for β_1H on W(100) at $\bar{\Gamma}$ of the two-dimensional Brillouin zone are $\nu_{wag} = 80$ meV, $\nu_{sym} = 130$ meV, and $\nu_{asy} = 160$ meV. Corresponding modes for β_1D on W(100) are observed by EELS to be shifted down in energy by a factor of $\sqrt{2}$, as expected based on the mass ratio.

The height of the β_1H layer on W(100) determined by the ratio of parallel to perpendicular vibrational frequencies (given above) is in good agreement with the height obtained from LEED.[23] Based on these facts, one can argue that β_1H on W(100) appears to exhibit conventional behavior from the standpoint of EELS results. Later in this paper we will show that this system still offers some interesting and unexpected behavior.

Our experiments were performed using a modified Leybold–Heraeus ELS-22 electron energy-loss spectrometer. The modifications, which are described in detail elsewhere,[25,26] consist of expanding instrument capabilities in two ways: (1) modifications in the optics[25] and electronics which permit operation at several hundred eV impact energies, and (2) modifications in the spectrometer control unit which permit the monochromator and analyzer to be swept in tandem, permitting measurement of the elastic or inelastic scattering intensity as a function of incident kinetic energy.[26] The increased energy range permits LEED beams to be analyzed, which provides a very accurate means of aligning crystals in relation to the EELS scattering plane. High impact energies also enables EELS measurements of surface phonons[27] at large $k_{\parallel}$ (out to the edge of the two-dimensional Brillouin zone). The tandem sweep capability permits direct measurements of I vs V curves for elastic as well as inelastic peaks at high-energy resolution (<25 meV). Sample preparation and other experimental details have been described previously.[22]

III. RESULTS

Figure 1 displays an I vs V curve for β_1H on W(100) along the (11) direction. The calculated beam emergence for the (11) beam is 8.6 eV, but the energy at which rapid oscillations in reflected intensity terminate is ~9 eV. This behavior is typical of reflectance data; there appears to be an unexplained energy difference between calculated and measured "thresholds."[28] One of the more striking features of the spectra in Fig. 1 is the deep minimum in reflectance which occurs at 5.2 eV. The reflectance decreases to practically zero here, and this has interesting implications in relation to "dipole scattering" theory: does the inelastic scattering cross section also vanish or nearly vanish at this incident energy and if it does, what are the implications? Here we have an opportunity to test dipole scattering on the same crystal under identical conditions using the same spectrometer. The reflectance data of Fig. 1 exhibit a wide dynamic range of elastic cross section (over 50:1) which is attractive for such a test.

Figure 2 displays electron energy-loss spectra for β_1H on W(100) at several discrete energies in the range covered by Fig. 1, in particular, at 5.3 eV where the minimum reflectance occurs, and at other energies where the reflectance is

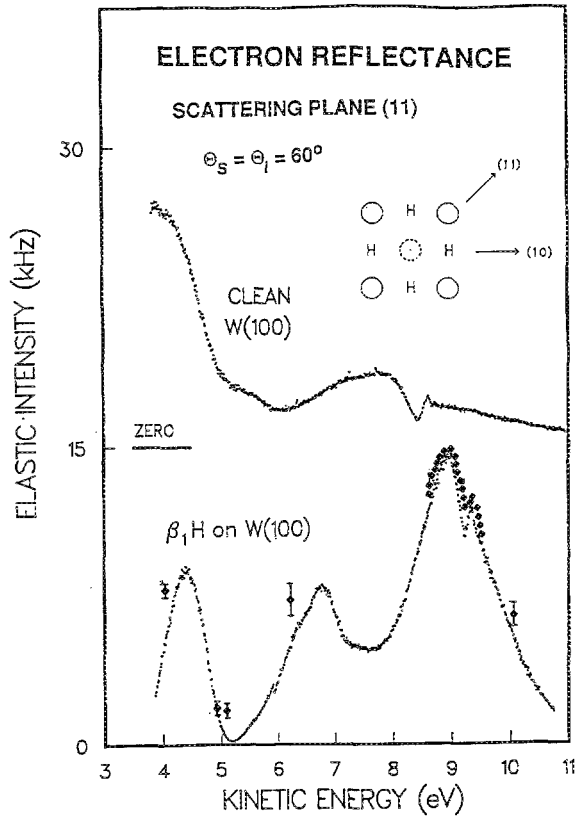

FIG. 1. Elastic reflectance data vs incident electron energy for clean W(100) at $T = 300$ K, and for β_1H on W(100). Scattering plane is along the (11) crystal axis; incident and reflected angles are 60° from the surface normal. Discrete points correspond to the measured 130-meV loss cross sections, taking into account the energy dependence (E^{-3}) introduced by the dipole scattering mechanism. Points around 8.5–9.5 eV represent a continuous scan of the 130-meV loss mode. Inset: real-space unit cell.

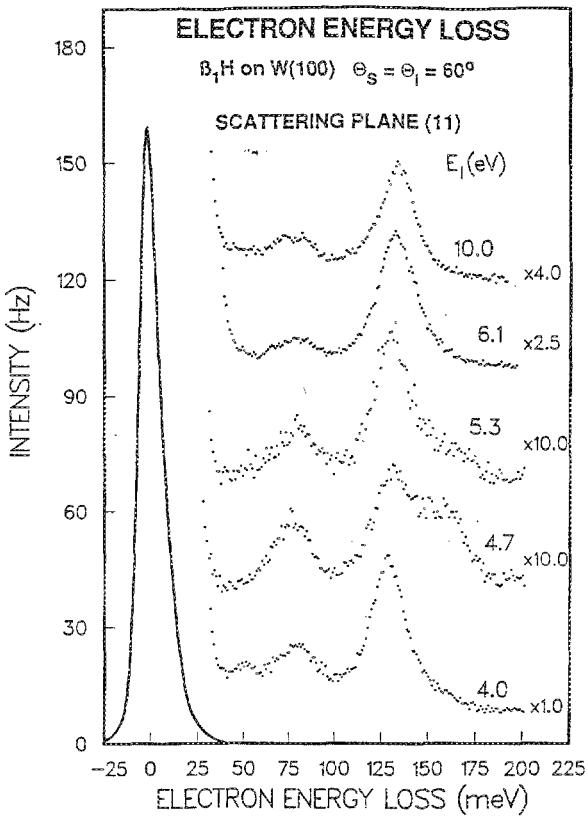

FIG. 2. Electron energy-loss spectra at selected incident energies E_i for β_1H on W(100). Scattering parameters are identical to those of Fig. 1. Scale factors are represented by numbers to far right.

higher. The spectra were taken under conditions (described in more detail below) which permit absolute intensities to be compared. Clearly, the relative cross sections vary with incident energy. In particular, at $E_i = 4.7$ eV, all three modes yield loss features of comparable intensity while at 9 eV (not shown) under the same scattering conditions, the 130-meV symmetric stretch mode dominates.

Target currents achieved by the electron monochromator are approximately independent of incident energy; in addition, the optics were retuned for each loss measurement, and during the reflectance measurement. Retuning is required to maintain optimum transmission through the spectrometer. We do not claim to have accurately determined the transmission function of our optics over the relevant energy range. However, ray-tracing analysis[25] of the lens system has established the fact that the electron beam focusing is well behaved for the lens voltages which yield maximum transmission. Based on the ray-tracing analysis, the transmission function is fairly constant ($\pm$ 10%) for the tuning conditions used over the entire kinetic energy range. Also, reflectance data obtained in the present studies agree reasonably well with data obtained by others using different instruments, suggesting well-behaved transmission functions. Once again, it is important to emphasize that in the present case, the same instrument is being used to compare relative dipole loss intensities with reflectance data, and to a first approximation, instrument transmission functions cancel out.

Inelastic intensities for the 130-meV symmetric stretch mode (dipole) are plotted on Fig. 1 taking into account the incident energy dependence introduced by the dipole scattering mechanism. Also shown are data corresponding to a continuous scan of the 130-meV loss intensity around $E_i = 9$ eV. These results establish the essential role the reflectance plays in determining the strength of dipole loss signals. A corresponding reflectance minimum (refer to inset of Fig. 3) occurs at $E_i = 4.2$ eV for scattering in the (10) crystal plane. Figure 3 displays the angular dependence of the symmetric stretch loss signal (for β_2D) at $E_i = 4.2$ and 15.5 eV. The elastic peak intensity (not shown) yields an angular dependence at 15.5 eV similar to that obtained for the symmetric stretch loss peak at this energy [full width at half-maximum (FWHM) $\sim 2°$], i.e., the symmetric stretch mode exhibits "dipole"-like behavior (even at $E_i = 15.5$ eV). However, at $E_i = 4.2$ eV the angular dependence is clearly not dipole. Corresponding (nondipole) dependence of the symmetric stretch mode of β_1H is observed at

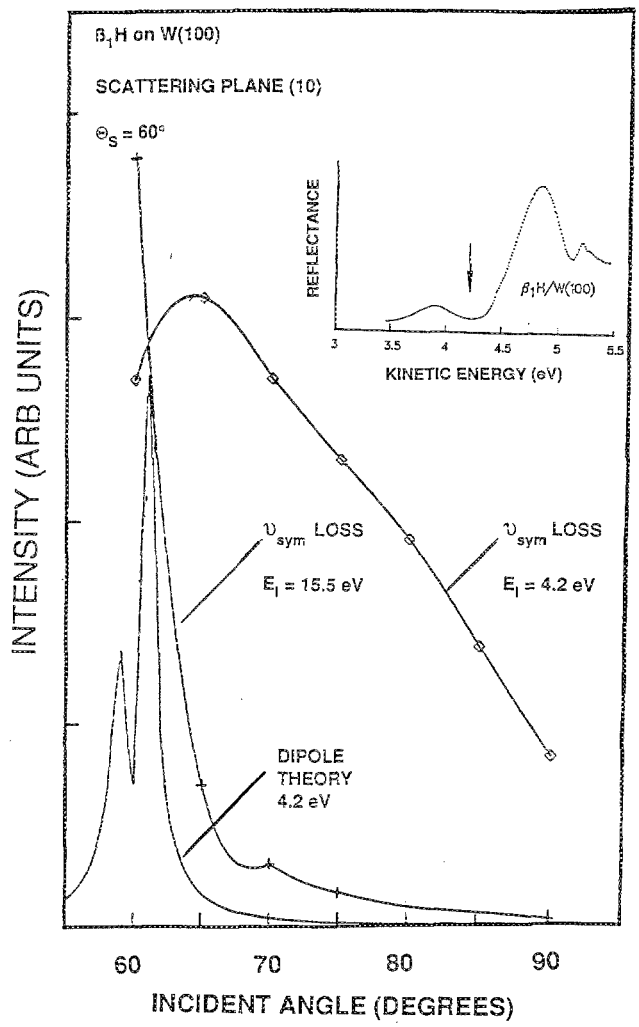

FIG. 3. Angular dependence of ν_{sym} of β_1H on W(100) at two incident energies. $\theta_s = 60°$, θ_i varies from 60° to 30°. Elastic peak angular dependence and calculated dipole loss angular dependence are also shown. Inset: elastic reflectance data vs incident electron energy for β_1H on W(100). Scattering plane is along the (10) crystal axis; incident and reflected angles are 60° from the surface normal. Arrow represents calculated LEED emergence energy.

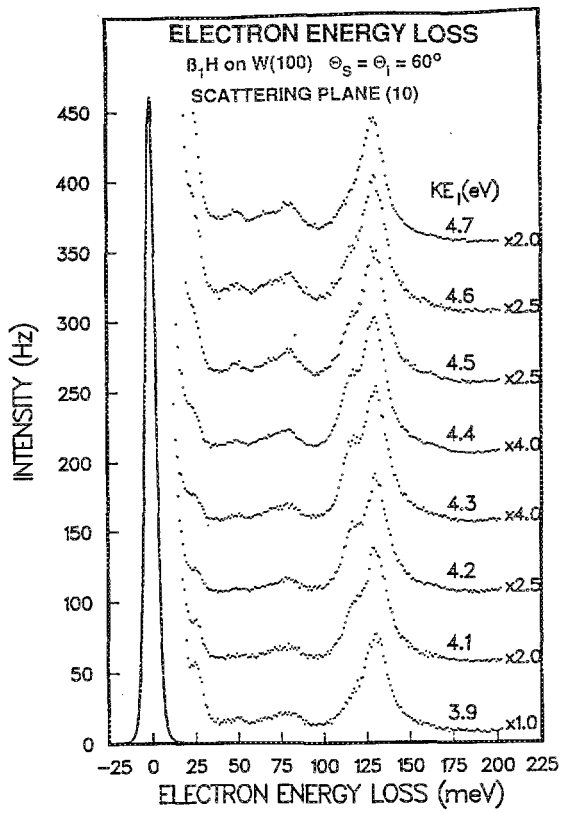

FIG. 4. Electron energy-loss spectra at selected incident energies E_i for β_1H on W(100). The new 118-meV loss peak is clearly apparent at $E_i = 4.3$ eV but is only observed in the wing of the 130-meV loss peak at other incident energies.

$E_i = 5.3$ eV for scattering along the (11) direction. In both of these specific cases, the *specular* scattering losses result from the *impact scattering* mechanism at incident energies corresponding to reflectance minima.

We now consider a second example in which a combination of LEED, surface reflectance, and EELS has yielded useful information. Figure 4 displays a series of EELS spectra for β_1H on W(100) covering impact energies around the 4.3-eV reflectance minimum. In these experiments, the (10) crystal axis was precisely aligned along the scattering plane using the (10) LEED beam, and the reflectance along this crystal azimuth, shown as an inset in Fig. 3, was determined using our EELS optics operating in the *I–V* mode set at the elastic peak.

The loss spectra exhibit an interesting new phenomena. In the impact energy range extending from 4.1 to 4.5 eV, a new loss peak at 118 meV emerges from the wing of the 130 meV (symmetric stretch peak) and then vanishes. Corresponding behavior is observed for β_2D (an 83-meV peak is observed). Curve fitting of the loss peaks[22] suggests that the cross section of the 118-meV peak is approximately constant, and that the striking change observed in the spectra is due primarily to the pronounced decrease in the 130-meV mode (dipole) cross section associated with the minimum in reflectance apparent in Fig. 3. This particular minimum occurs very near the calculated beam emergence energy, and the reflectance minima are probably a direct result of the beam emergence.

The origin of the 118-meV mode has been the subject of some debate. Off-specular EELS measurements[22,24] have clearly established the fact that the 118-meV mode behaves as though it is caused by impact scattering; this favors its assignment to a parallel vibration, but in reality, as in the two examples just discussed, it results from a perpendicular mode. Additional experimental results[24] [which have now established the dispersion of the surface vibrational modes of β_1H on W(100) as a function of $k_\parallel$ along the $\bar{M}$ direction] coupled with extensive lattice dynamical modeling of the system, now appear to have resolved the origin of this mode. The β_1H phase on W(100) contains two hydrogen atoms per tungsten unit cell; this allows as many as six adsorbate vibrational modes. The 118-meV mode is one of the fundamental H modes (optical mode) which is observable under beam emergence conditions. These results are discussed in detail elsewhere.[24]

As a third and final example of a case in which the ability to compare vibrational intensities is important, we mention recent work on the H/Nb system. EELS studies[29] of H on Nb(100) have shown that adsorbed H atoms chemisorb in tetrahedral sites below the surface. These sites exhibit a novel reversible temperature-dependent behavior which governs the admission of H into the bulk. Direct comparisons between H vibrational intensities associated with other Nb surfaces and Pd coated Nb surfaces will be extremely useful in testing uptake kinetics models for the H/Nb systems which invoke a "surface valve" mechanism based on these subsurface sites.

IV. SUMMARY

We have attempted to illustrate, using two specific examples, the utility of combining three complementary electron scattering probes of the surface in a single instrument. The primary features of this combination which account for the potential for unique experiments include (1) the ability to precisely align a crystal mirror plane for EELS experiments by using the EELS optics in a LEED mode; (2) the ability to make absolute comparisons between electron reflectance and dipole losses as a function of energy (because the same electron optics are used with the same lens voltage operating mode), and (3) the convenience of performing a reflectance *I–V* measurement before conducting EELS studies to determine which incident energies will yield the best dipole loss counting rates. By combining (specular) reflectance measurements with specular and off-specular EELS measurements, it is possible to determine the *impact scattering* contribution to loss intensities of perpendicular vibrations detected in *specular scattering geometry*. Under certain scattering conditions losses measured in specular scattering may be dominated by impact scattering mechanisms and care must be exercised in assigning mode symmetry based on the "dipole" scattering selection rule.

ACKNOWLEDGMENTS

This work was sponsored by the U. S. Air Force Office of Scientific Research under Grant No. AFOSR-86-0109, and by the Robert A. Welch Foundation.

[1]E. G. McRae, Rev. Mod. Phys. **51**, 541 (1979).
[2]J.-M. Baribeau, J.-D. Carette, P. J. Jennings, and R. O. Jones, Phys. Rev. B **32**, 6131 (1985); R. O. Jones, P. J. Jennings, and O. Jepsen, *ibid.* **29**, 6474 (1984).
[3]R. C. Jaklevic and L. C. Davis, Phys. Rev. B **26**, 5391 (1982); R. C. Jaklevic, *ibid.* **30**, 5494 (1984).
[4]R. E. Dietz, E. G. McRae, and R. L. Campbell, Phys. Rev. Lett. **45**, 1280 (1980).
[5]E. Evans and D. L. Mills, Phys. Rev. B **5**, 4126 (1971).
[6]A. A. Lucas and M. Sunjic, Phys. Rev. Lett. **26**, 229 (1971); Prog. Surf. Sci. **2**, 2 (1972).
[7]D. M. Newns, Phys. Lett. A **60**, 461 (1979).
[8]F. Delanaye, A. Lucas, and G. D. Mahan, Surf. Sci. **70**, 629 (1978).
[9]D. Sokcevic, Z. Lenac, R. Brako, and M. Sunjic, Z. Phys. B **28**, 677 (1977).
[10]B. N. J. Persson, Solid State Commun. **24**, 573 (1977).
[11]B. M. Hall, S. Y. Tong, and D. L. Mills, Phys. Rev. Lett. **50**, 1277 (1983); S. Y. Tong, C. H. Li, and D. L. Mills, Phys. Rev. B **24**, 806 (1981).
[12]A. J. Melmed and W. R. Graham, Appl. Surf. Sci. **11/12**, 470 (1982).
[13]M. K. Debe and D. A. King, Phys. Rev. Lett. **38**, 708 (1977); J. Phys. C **10**, L303 (1977).
[14]T. E. Felter, R. A. Barker, and P. J. Estrup, Phys. Rev. Lett. **38**, 1138 (1977); R. A. Barker, P. J. Estrup, F. Jona, and P. M. Marcus, Solid State Commun. **25**, 375 (1978).
[15]R. A. Barker and P. J. Estrup, Phys. Rev. Lett. **41**, 1307 (1978).
[16]D. A. King and G. Thomas, Surf. Sci. **92**, 201 (1980).
[17]R. F. Willis, Surf. Sci. **89**, 457 (1979).
[18]M. A. Passler, B. W. Lee, and A. Ignatiev, Surf. Sci. **150**, 263 (1985).
[19]R. Biswas and D. R. Hamann, Phys. Rev. Lett. **56**, 2291 (1986); M. Weinert, A. J. Freeman, and S. Ohnishi, *ibid.* **56**, 2295 (1986).
[20]I. Stensgaard, L. C. Feldman, and P. J. Silverman, Phys. Rev. Lett. **42**, 247 (1979); L. C. Feldman, P. J. Silverman, and I. Stensgaard, Surf. Sci. **87**, 410 (1979).
[21]W. Ho, R. F. Willis, and E. W. Plummer, Phys. Rev. B **21**, 4202 (1980).
[22]J. P. Woods and J. L. Erskine, Phys. Rev. Lett. **55**, 2595 (1985).
[23]Recent EELS data (see Ref. 22) and data presented in the present paper show that a strong 118-meV mode exists for β_1H on W(100). The suggestion that this mode could correspond to the asymmetric stretch mode leads to a H height of 1.74 Å, which differs significantly from the height (1.17 Å) suggested by LEED (Ref. 18) and calculations (Ref. 19). More extensive experimental data and lattice dynamical analysis of the dispersion of β_1H modes on W(100) (Ref. 24) now suggest that the 118-meV mode corresponds to out of phase perpendicular vibrations of nearest-neighbor H atoms (optic mode).
[24]J. P. Woods, A. D. Kulkarni, J. L. Erskine, and F. W. deWette, Phys. Rev. B (in press).
[25]R. L. Strong and J. L. Erskine, Rev. Sci. Instrum. **55**, 1304 (1984).
[26]J. P. Woods and J. L. Erskine (to be published).
[27]R. L. Strong and J. L. Erskine, Phys. Rev. B **31**, 1537 (1985); Phys. Rev. Lett. **54**, 346 (1985).
[28]J. M. Baribeau and D. Roy, Surf. Sci. **166**, 234 (1986).
[29]Y. Li, J. L. Erskine, and A. C. Diebold, Phys. Rev. B **34**, 5951 (1986).